Available online at www.sciencedirect.com
SCIENCE DIRECT®
Catalysis Today 101 (2005) 359–367
CATALYSIS TODAY
www.elsevier.com/locate/cattod

Supported photosensitizers as new efficient materials for gas-phase photo-oxidation

V. Latour [a], T. Pigot [a], P. Mocho [b], S. Blanc [a], S. Lacombe [a,*]

[a] *Laboratoire de Chimie Théorique et de Physico-Chimie Moléculaire, UMR CNRS 5624, FR 2606, Faculté des Sciences, BP 1155, 64013 PAU cedex, France*
[b] *Laboratoire de Thermique, Energétique et Procédés, UPPA, CURS, BP 1155, 64013 PAU cedex, France*

Available online 7 April 2005

Abstract

The photosensitised oxidation of dimethylsulfide in the gas phase was carried out for the first time on original silica materials in a flow reactor and under visible light irradiation. The photocatalysts were prepared either by physisorption of two different photosensitizers, 9,10-dicyanoanthracene or 9,10-anthraquinone on commercial silica beads, or by incorporation of 9,10-dicyanoanthracene in sol–gel monoliths. Oxidation products are mainly sulfoxide, sulfone and disulfide, and it is assumed that singlet oxygen is the most probable reactive oxygen species.

These materials display several advantages as they are activated by visible light, and they act as very efficient traps for partially oxidized products. Accordingly, the gas-flow at the outlet of the photocatalytic device is free of any toxic or nauseous product for several days. As soon as products appear in the gas flow, the catalyst is deactivated, but the silica beads can be easily regenerated by mild thermal treatment under controlled conditions.

With regard to the photo-oxidative efficiency, our results point out the influence of the properties of the silica support itself, such as transparency, homogeneity and specific surface area. The adsorption capacity of the material is a crucial parameter, as the most DMS adsorbing material is also the most efficient.

Keywords: Alkylsulfide; Photo-oxidation; Photosensitization; Gas–solid reactions; Supported photocatalysts

1. Introduction

Supported photosensitizers have been known for a long time and have mainly been used for solution reactions as they are easily recovered from the solvents, avoiding difficult purification steps of the reaction products [1–18]. Moreover, insoluble photosensitizers, when supported on inert matrices, can also be used under heterogeneous conditions in some solvents where the homogeneous reaction cannot be carried out [19–21]. However, gas-phase photo-oxidation of organic compounds in the presence of oxygen has been seldom described with such materials [22,23]. Usually, these gas-phase reactions are carried out over the well-known photocatalyst, titanium dioxide (TiO_2) in its anatase form [24,25]. This inexpensive, stable and non-toxic photocatalyst is highly efficient for the oxidation of most organic molecules. Its main drawbacks are its weak light adsorption in the visible range (only 3–5% of solar emission), its low surface area (50 $m^2\ g^{-1}$ for the often used DEGUSSA P25), and its difficult handling as a powder in gas-phase reactors. Accordingly, a lot of research is devoted to the modification of TiO_2, in order to improve its absorption spectrum towards longer wavelengths, and to the preparation of more convenient or adsorbing TiO_2-based materials.

We address in this paper, the preparation, characterization and use of photoactive materials based on aromatic photosensitizers, such as 9,10-dicyanoanthracene (DCA) and anthraquinone (ANT), supported on silicagel matrix for the gas-phase photo-oxidation of dimethylsulfide under visible irradiation. These two photosensitizers have been chosen for their known efficiency to convert sulfides mainly

* Corresponding author. Tel.: +33 5 59 407 579; fax: +33 5 59 407 585.
E-mail address: sylvie.lacombe@univ-pau.fr (S. Lacombe).

0920-5861/$ – see front matter © 2005 Elsevier B.V. All rights reserved.
doi:10.1016/j.cattod.2005.03.023

to sulfoxides in acetonitrile [26,27], and for their sensitivity at 420 nm, i.e., in the short wavelengths side of the visible spectrum.

Different kinds of interactions between the aromatic photosensitizers and the silicagel matrix may be considered. Weak interactions are expected upon physisorption of the dye on silicagel or upon its encapsulation in the silica network during sol–gel synthesis, while chemisorption of the photosensitizer molecule on surface silanols implies its functionalization with a spacer bearing a trialkoxysilyl (–$Si(OR)_3$) or trichlorosilyl (–$Si(Cl)_3$) group [17,18]

In the following, we only prepared the first kind of physisorbed materials, with the initial aim of studying the feasibility of gas-phase photo-oxidation reactions and of comparing the efficiency of the different materials under similar conditions.

2. Experimental

DCA was purchased from Kodak and used as received. ANT was purchased from Aldrich and crystallized in ethanol before use. Chloroform, acetonitrile and methanol were purchased from Aldrich, and were HPLC grade. In order to conveniently handle the catalysts in the gas-phase reactor, no powders were used but instead either large particle-silicagel from Acros (particle size 3–6 mm, surface area 330 $m^2\ g^{-1}$, average pore diameter 2–4 nm) called CB materials in the following, or sol–gel monoliths prepared in the laboratory.

DCA-CB and ANT-CB were prepared by mixing CB silica-gel, pretreated at 100 °C for 12 h in a chloroform solution of DCA (100 g of CB in 1 l of 1.73×10^{-3} mol l^{-1} solution) or of an acetonitrile solution of ANT (50 g of CB in 100 ml of 10^{-3} mol l^{-1} solution). The mixture was stirred on an ellipsoidal table for 12 h at room temperature, and the silicagel filtered and dried at 100 °C for 12 h. From the drop of the photosensitizer concentration in the solution before and after adsorption, the DCA loading on DCA-CB is 4.36×10^{-6} mol g^{-1}, while the ANT loading on ANT-CB is 4.45×10^{-6} mol g^{-1}.

Clear and crack-free silica monoliths loaded with DCA (DCA-SG) were obtained by the conventional hydrolysis and condensation of tetramethylorthosilicate (TMOS, Aldrich, 99%) in the presence of methanol, under acidic conditions. Samples of different porosity can be obtained, depending on the TMOS/methanol/water ratio. In this work, it was chosen as 1/5/4, i.e., an initial stoichiometric ratio of water to TMOS. A 6.31×10^{-5} mol l^{-1} solution of DCA in methanol was added to water (reverse osmosis, 5–10 μS cm^{-1}) acidified by hydrochloric acid until pH 3 and TMOS was added in one step. This solution was stirred magnetically for 2 min. Samples of the sol were closed in polypropylene Eppendorf® microtubes. Gelation was achieved within 10 days in an oven at 50 °C. The microtubes were then opened in order to dry the gels at atmospheric pressure for 10 days at 30 °C, 6 h at 50 °C and 60 h at 80 °C, after which the samples were kept in the closed tubes until use. Residual water and methanol are present in the dried monoliths. From the weight of the monoliths and the initial concentration of DCA in the methanol solution, the DCA concentration in DCA-SG is calculated to be 2.08×10^{-7} mol g^{-1}.

Nitrogen adsorption and desorption isotherms of the materials were measured at 77 K on a Micromeritics ASAP 2010 Micropore nitrogen adsorption apparatus. Absorbance spectra of solutions and Diffuse Reflectance UV (DRUV) spectra of the previously prepared ground materials were recorded on a Varian Cary 5 spectrometer. The DRUV spectra were recorded with the "Praying Mantis" accessory (Harrick). For each sample, the height of the sampling cup is adjusted to optimise the reflection signal. DRUV spectra of loaded silica gels were recorded in reflectance units against unloaded samples prepared under the same conditions and were transformed in Kubelka–Munk remission function $F(R)$:

$$F(R) = \frac{(1-R)^2}{2R} = \frac{k}{S} = \frac{\varepsilon c}{S} \quad (1)$$

where S stands for the scattering coefficient (depending on the size and form of the particles), ε the molar absorption coefficient of the analyte and c its molar concentration. The Kubelka–Munk transformation thus converts a reflectance spectrum into a spectrum similar to a conventional absorbance spectrum for solution samples [28].

The fluorescence and excitation spectra of DCA-SG were recorded with a Perkin-Elmer spectrofluorimeter LS50B and a homemade sample holder.

For the gas-phase photo-oxidation experiments, a single-path flow reactor (Fig. 1) was used. A stable DMS (Aldrich) concentration is delivered by a diffusion cell [29,30] at −5 °C where a mass flowmeter supplies a constant flow of pure oxygen (AIR LIQUIDE, Alphagaz1, 67 ml min^{-1}). Under these conditions, the DMS concentration is 102 ppmv (283 mg m^{-3}). The gas flows through a cylindrical (internal diameter 1.5 cm) pyrex reactor thermo-regulated at 20 °C and closely packed with 3 g of the commercial beads or monoliths. The pyrex reactor is located inside a modified

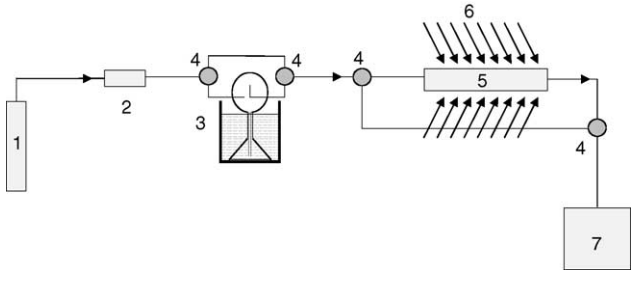

Fig. 1. Scheme of the single-path gas-phase flow reactor. (1) Pressured oxygen tank; (2) mass flowmeter; (3) diffusion cell in a thermo-regulated bath; (4) three-path Teflon valves; (5) photocatalytic reactor (thermo-regulated pyrex tube); (6) 420 nm fluorescent lamps from a modified Rayonet® reactor; and (7) GC-FID chromatograph.

horizontal Rayonet® reactor equipped with 14 RPR-4190 lamps (emission maximum at 420 nm). The gas outlet is directly sampled by a pneumatic valve located on the injection port of a VARIAN 4800 chromatograph equipped with a Chrompack column CPSil-5CB (30 m, 0.25 mm, 1 μm). The gas flow is analysed every 10 min and the concentration of DMS or of its oxidation products is thus followed over the whole experiment after identification of the oxidation products by comparison with pure standards or analysis by GC–MS. Alternatively, a Varian CP-4900 micro-GC with a thermal conductivity detector may be used to detect sulfur dioxide, carbon dioxide or water in the effluent. At the end of irradiation, the materials are heated at 80 °C in the reactor under oxygen flow, and the gaseous components are concentrated on a Carboxen SPME fibre, which is then desorbed in the injector of a HP 5973 GC–MS chromatograph (column SPB35, 60 m, 0.32 mm, 1 μm) for analysis of the oxidation products. Finally, the materials after irradiation are stirred first for 4 h in acetonitrile, and then after separation from the solvent, 4 h in deionized water. The acetonitrile solution is analysed by GC–MS for identification of desorbed organic products, while the aqueous extract is analysed by ion exchange chromatography in the suppressed conductivity mode on a Dionex DX-20 chromatograph equipped with an AS9-HC (4 mm) column.

3. Results

We focused these experiments on the comparison of the efficiency of the materials DCA-CB, ANT-CB and DCA-SG for DMS photo-oxidation. They were thus carried out with about 3 g of materials, and with the same DMS concentration, oxygen flow and irradiation under a dynamic regime. In other words, DMS is constantly supplied to the reactor all along the experiment.

3.1. Photo-oxidation experiments

In a first step, DMS is adsorbed in the dark on the material until the equilibrium DMS concentration (C_{eq}) is reached in the gas flow. The integration of the curve giving the DMS concentration in the gas flow against time or breakthrough curve (Fig. 2) allows the calculation of adsorbed DMS per gram of material (Table 1). In the dark, the DMS adsorption properties of DCA-CB and ANT-CB are of the same order of magnitude (5.4 and 7 mg g^{-1}, respectively), and noticeably weaker than that of the DCA-SG material (211 mg g^{-1}). These results, illustrated by the breakthrough curves of Fig. 2, are consistent with the surface area of the materials determined by BET: 330 $m^2 g^{-1}$ for CB materials and 700 $m^2 g^{-1}$ for the SG one. Moreover, the nitrogen adsorption isotherm of DCA-SG displays a type IV hysteresis loop characteristic of a mesoporous material [31] with mean BJH pore sizes around 22 nm, while for the CB materials the mesopore sizes are found between 2 and 4 nm.

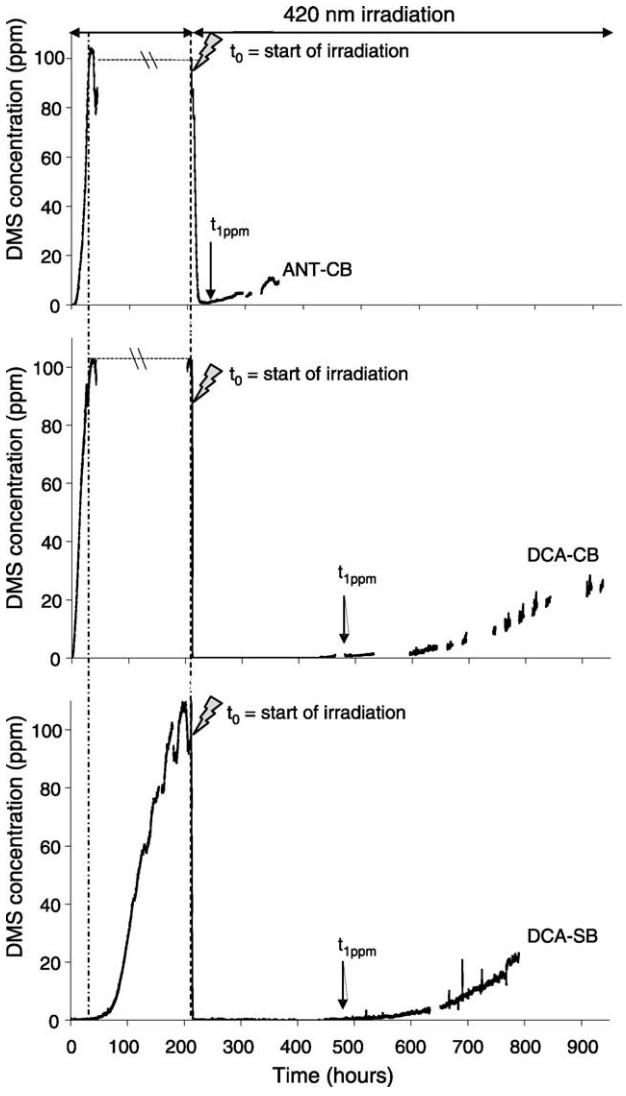

Fig. 2. Breakthrough curves of DMS on different photosensitizing materials: top ANT-CB; middle DCA-CB; bottom DCA-SG.

Table 1
Characteristics of the materials used for the photo-oxidation experiments

	Surface area ($m^2 g^{-1}$)	Photosensitizer concentration (mol g^{-1})	Adsorbed DMS (mg g^{-1})	$t_{1\ ppm}$	TON
DCA-CB	330	4.34×10^{-6}	5.4	242	310
ANT-CB	330	4.46×10^{-6}	7	9	11
DCA-SG	700	2.08×10^{-7}	211	295	7500

Adsorbed DMS is calculated by integration of the curve giving the DMS concentration in the gas flow against time in the dark. $t_{1\ ppm}$ refers to the time between the start of irradiation t_0 and the time when the DMS concentration in the gas flow is 1 ppm. TON is the turnover number (see text).

With the three materials, once C_{eq} is reached, the lamps are switched on, and the DMS concentration in the flow immediately drops to zero and only slowly increases (Fig. 2). We have chosen to compare the materials by the measured time to detect again a DMS concentration of 1 ppm ($t_{1\ ppm}$) in the gas flow. It may be observed that $t_{1\ ppm}$ is much shorter with ANT-CB (9 h) than with the DCA-based materials DCA-CB (242 h, 10 days) and DCA-SG (295 h, 12 days).

From the value $t_{1\ ppm}$, a turnover number (TON) is defined as the number of DMS molecules consumed between the start of illumination (t_0) and $t_{1\ ppm}$ divided by the number of photocatalytic sites [32]. As in homogeneous photosensitization, the number of active sites is defined as the number of photosensitizer molecules (in its ground state) deposited on the material.

$$\text{TON} = \frac{\text{Number of moles DMS consumed between } t_0 \text{ and } t_{1\,ppm}}{\text{Number of moles of DCA}} \quad (2)$$

$$\text{TON} = \frac{DC^0_{DMS}(t_{1\,ppm} - t_0)10^{-6} \times 60}{C^0_{DCA} m}$$

where D is the oxygen flow (ml min^{-1}), C^0_{DMS} the initial DMS concentration (mol m^{-3}), $t_{1\ ppm}$ the time when the DMS concentration under irradiation reaches 1 ppm (h), t_0 the time of the start of irradiation (h), C^0_{DCA}: DCA concentration in the material (mol g^{-1}) and m the mass of material in the reactor (g).

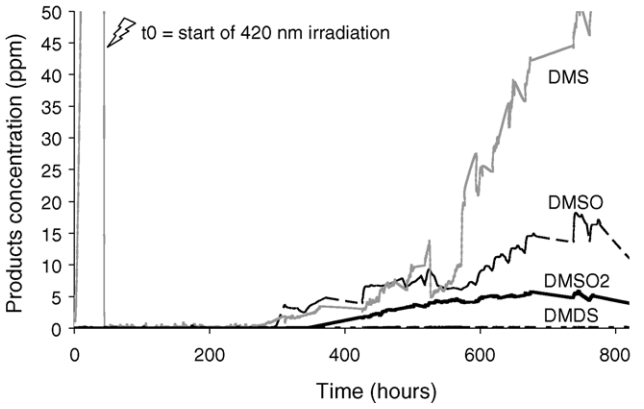

Fig. 3. Concentration of oxidation products in the gas phase during irradiation over DCA-CB.

Accordingly, the better oxidation efficiency is achieved with DCA-SG (TON 7500). The commercial silicagel beads, DCA-CB, are less efficient (TON 310) as a higher DCA concentration in the material is necessary to obtain $t_{1\ ppm}$ of the same order of magnitude. ANT-CB appears to be only weakly efficient for DMS oxidation in the gas phase (TON 11).

During the irradiation, no oxidized product is detected in the gas phase until the DMS concentration begins to increase. At this time, the concentration of dimethylsulfoxide (DMSO), dimethylsulfone ($DMSO_2$) and dimethydisulfide (DMDS) also increases (Fig. 3 for DCA-CB).

Table 2
Oxidation products detected either in the gas phase or by desorption of the irradiated materials in different solvents

Treatment	Oxidation products	Material				
		DCA-CB		DCA-SG		ANT-CB
		After 8 days	After 30 days	After 8 days	After 24 days	After 8 days
Desorption in the gas phase under irradiation	DMSO	+	+++	+	++	++
	$DMSO_2$	+	++	+	++	+++
	DMDS	+	+	+	+	+++
Desorption in the gas phase in the dark by heating at 80 °C	DMSO	Yes		Yes		
	$DMSO_2$	Yes		Yes		Yes
	DMDS	Yes		Yes		Yes
	DTP	Yes		Yes		Yes
	Formaldehyde	Yes		–		–
	DMTS	Yes		–		Yes
	MMTS	–		–		Yes
	Methanethiol	–		Yes		Yes
Desorption in acetonitrile	$DMSO_2$	Yes		Yes		Yes
	Acetic acid	–		Yes		Yes
	MMTS	–		–		Yes
Desorption in water	Acetate	Traces		–		–
	Formiate	–		–		–
	Methanesulfonate	+		–		Traces
	Sulfate	–		–		–
	Sulfite	Traces		–		–

+++: Main product, ++: second main product, +: less abundant product, –: absence, yes: detected product.

However, their relative concentration depends on the irradiation time as some products are desorbed more easily than others. Other oxidized products are desorbed from the material at the end of irradiation, either by heating the reactor at 80 °C, or by two consecutive extractions in acetonitrile and water. The products detected on the materials under these different conditions are compared in Table 2. With all the materials, the main reaction products are DMSO, $DMSO_2$ and DMDS, the former being the most abundant. However, other by-products are also possibly desorbed in trace amounts: 2,5-dithiapentane (DTP, $CH_3SCH_2SCH_3$) from DCA-CB and DCA-SG, methanethiol from DCA-SG, formaldehyde and dimethyltrisulfide (DMTS) from DCA-CB and ANT-CB, methyl methanethiosulfonate (MMTS, $CH_3SS(O)_2CH_3$) only from ANT-CB. Acidic products, such as acetic acid and mainly methanesulfonic acid are also detected when using DCA-CB or ANT-CB, but the yields in acidic products remain very low (<2%). No sulfur dioxide (SO_2) or carbon dioxide (CO_2) is detected when analyzing the gas flow with a chromatograph equipped with thermal conductivity detectors.

3.2. Evolution of the material during irradiation

Besides the structural characterization of the porous silica gels by BET, the DRUV or fluorescence analysis of the photosensitizer on the support has been carried out before and after irradiation. None of these latter methods was used for a quantitative determination, but rather for qualitative indications. The DRUV spectrum of DCA-CB before irradiation is similar to the absorbance spectrum of DCA in solution (Fig. 4). However, the band around 260 nm is strongly distorted in the DRUV spectrum because of baseline absorption of silica at short wavelength on one hand, and of the fluorescence emission of DCA on the other hand. Nonetheless, it is obvious from the spectra after irradiation that the DCA band centred at 400 nm is modified after 13 irradiation days; the band intensity strongly decreases and the signal exhibits a noticeable shoulder towards longer wavelength (450 nm, see right part of the spectra in Fig. 4). At the same time, a strong intensity band appears between 200–220 nm, which can tentatively be assigned to oxidation products (DMSO, $DMSO_2$, DMDS) adsorbed on the material. When the irradiation time is longer (19 days, Fig. 4), the intensity of the DCA bands still decreases, and it is almost absent after 33 days, indicating the photosensitizer consumption.

Further experiments, with short irradiation time (≤13 days), were carried out on the same kind of materials and confirm this spectral evolution. However, the initial DRUV signal of DCA may be restored by heating the irradiated material DCA-CB for 12 h at 60 °C under vacuum. Under these conditions, the adsorbed oxidation products are mostly evacuated, the intensity of the DRUV band between 200 and 220 nm strongly decreases, while the intensity of the 400 nm band increases with disappearance of the 450 nm shoulder. This thermal regeneration of the material proved to be efficient, provided the irradiation time was not too long (≤13 days), and five successive cycles adsorption–irradiation–thermal regeneration could thus be achieved.

As for DCA-CB, the DRUV spectra of ANT-CB depend on the irradiation time with disappearance of ANT signals at long irradiation times (170 h). After shorter irradiation times (89 h) and heating of the material under vacuum at 60 °C for several days, the initial ANT signals may be partly restored in the DRUV spectrum and another irradiation cycle could be achieved after this treatment.

According to these results, for DCA-CB, the detection of DMS and of its oxidation products in the gas flow after about 10 days (242 h) of irradiation is related to the evolution of the

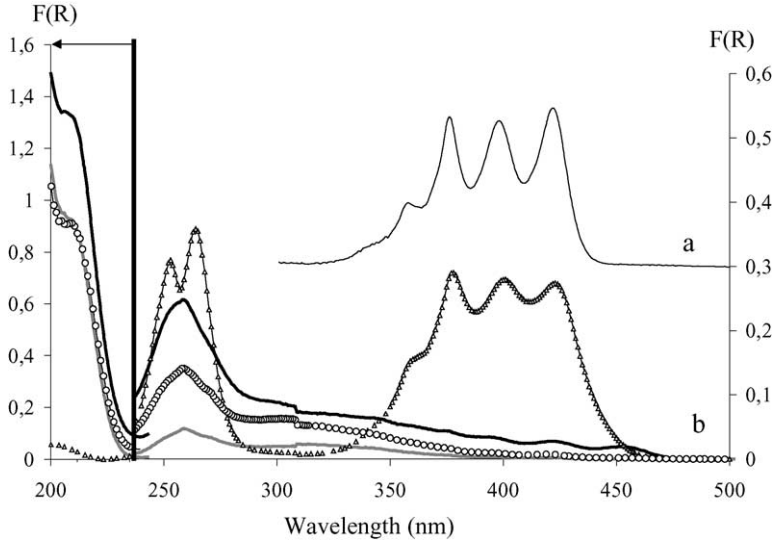

Fig. 4. (a) Absorbance spectrum of DCA in MeOH solution. (b) DRUV spectrum of DCA-CB before irradiation (triangles), after 13 days of irradiation (black line), after 19 days of irradiation (circles) and after 33 days of irradiation (grey line).

DRUV spectrum. At this irradiation time, this evolution is reversible and the spectral characteristics of DCA may be restored by suitable thermal treatment of the material. If irradiation further goes on, DCA is consumed as shown by the DRUV spectrum while the concentration of DMS and its oxidation products increases in the gas flow. In other words, in order to keep a material suitable for reactivation, irradiation has to be stopped as soon as DMS and its oxidation products are detected in the flow. Hence, the DMS concentration of 1 ppm in the flow was chosen for the calculation of TON.

Although the intensity of the DCA bands in the DRUV spectrum of DCA-SG are very weak before irradiation because of the low photosensitizer concentration in this material, a noticeable intensity decrease is observed after irradiation as previously, indicating some partial consumption of DCA. Therefore, DCA-SG is better analysed by fluorescence spectroscopy (Fig. 5). In this case, the monolith sample is directly set up inside the sample holder at the common focal point of the excitation and emission beams for maximizing the signal output. It is thus difficult to compare different spectra on quantitative grounds, as the position of the sample is not reproducible. Nonetheless, some useful indications may be drawn from these spectra. First, no excimer signal, characterized in the emission spectrum by a broad unstructured band at longer wavelength, is detected for this material either before or after irradiation. Upon irradiation, the relative band intensity of the emission spectra is modified, as the first component appears slightly shifted to lower energy by about 6 nm before irradiation; this effect may be assigned to re-absorption in this more concentrated sample. After irradiation, a weak intensity band is also observed in the emission spectrum before the DCA signal between 390 and 420 nm, and probably arises from a fluorescent decomposition product of DCA. The excitation spectra are roughly similar before and after irradiation although a weak broadening of the DCA band both at short and long wavelengths is noticed.

The irradiated monoliths have been washed in acetonitrile and water to extract the oxidation products, and it is important to note that the DCA emission and excitation spectra are not modified at all after this treatment; this implies that the fluorescent molecule is well encapsulated inside the monolith material and cannot be desorbed in solution.

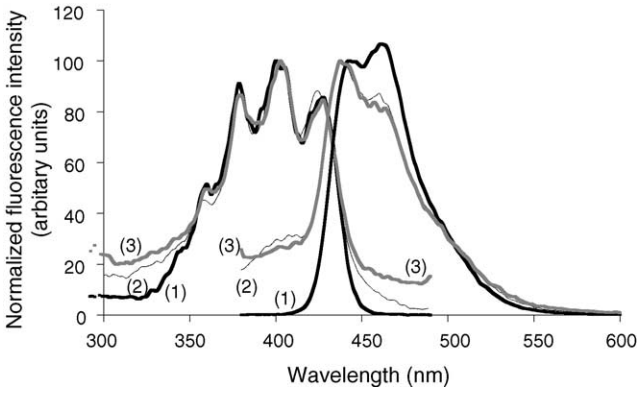

Fig. 5. Emission (λ_{exc} 370 nm) and excitation (λ_{em} 440 nm) spectra normalized at 440 nm of DCA-SG before irradiation (1, black thick line), after irradiation (2, black thin line) and after washing in acetonitrile and water (3, grey thick line).

4. Discussion

DCA and ANT are well-known photosensitizers, both able to sensitize in the presence of oxygen the formation of either singlet oxygen or superoxide anion, depending on the conditions (solvent, substrate, concentration ...) [33–35]. Our results extend for the first time this efficiency to gas–solid oxidation reactions. Actually, DMS is converted mainly to dimethylsulfoxide, dimethylsulfone and dimethyldisulfide with the three tested materials. The calculated turnover number (TON) is in every case superior to one, which is indicative of a catalytic (non-stoichiometric) reaction; each photosensitizer molecule converts several molecules of DMS before deactivation of the material. However, the best results are by far obtained with the DCA-based materials, DCA-CB (TON 310) and DCA-SG (TON 7500), while ANT-CB is not very efficient (TON 11). This poor gas–solid activity may tentatively be assigned to the weak molar absorption coefficient of ANT at 420 nm (50 mol l^{-1} cm^{-1}) relative to DCA (11 150 mol l^{-1} cm^{-1}).

It may also be concluded from these experiments that the best efficiency is achieved for the lowest photosensitizer concentration in the material (2.08×10^{-7} mol g^{-1} for DCA-SG). In the fluorescence emission spectra of DCA-CB (DCA concentration 4.34×10^{-6} mol g^{-1}), a weak excimer band was detected and its relative intensity was dependent on the sample position in the sample holder, demonstrating the heterogeneity of DCA deposit in the material. The presence of this excimer in DCA-CB probably partly deactivates some of the photosensitizer molecules, limiting its oxygen activation ability.

The comparison between DCA-CB and DCA-SG points out the importance of the adsorption step for the photo-oxidation efficiency and highlights the properties of the silica material itself. Indeed, from the calculation of adsorbed DMS in the dark (Table 1), DCA-SG proved to be a much better DMS adsorbant (211 mg g^{-1}) than the CB beads (5 mg g^{-1}). Moreover, the sol–gel monoliths are much more transparent than the CB beads, and owing to their preparation, the photosensitizer molecules are uniformly distributed inside the porous network while for the CB materials, the fluorescence experiments indicate their less controlled distribution.

Finally, the main photo-oxidation products (DMSO, $DMSO_2$, DMDS) can be compared with those recently described by Vorontsov et al. for diethylsulfide photo-oxidation over irradiated TiO_2 in a flow reactor [36]. The detection in the gas phase of diethyldisulfide, acetaldehyde, ethylene, ethanol, as well as small quantities of sulfur

dioxide, carbon dioxide and C-oxidation products (C_2H_5–S–C(O)CH_3) was reported by the authors. Acetaldehyde, ethylene, ethanol and disulfide arise from C–S bond cleavage after formation of the sulfide radical-cation $C_2H_5SC_2H_5^{\bullet+}$ arising from the preliminary photochemical step. Desorption of the photocatalyst in isopropanol after irradiation yielded small amounts of the corresponding sulfoxide and sulfone, and oxidation at sulfur was thus shown to be only a minor pathway.

These literature data indicate that disulfide, DMDS, and its oxidized form, MMTS, could arise either from energy or electron transfer sensitization. However, DMTS, DTP, methanethiol, formaldehyde and formic acid, detected in trace amounts, are indicative of the involvement of radical species, as well as sulfonic acid issued from the addition of oxygen on thiyl radicals. These radical species imply C–S bond cleavage, starting from the initial radical-cation $CH_3SCH_3^{\bullet+}$.

$$CH_3SCH_3^{\bullet+} \rightarrow CH_3SCH_2^{\bullet} + H^+ \xrightarrow{O_2} CH_3SCH_2{-}O{-}O^{\bullet} \rightarrow \rightarrow \rightarrow CH_3S^{\bullet} + HCHO$$

In our case, the product distribution is obviously different and do not vary significantly with the three materials. Minor products arising from C–S bond cleavage are DMTS, DTP, methanethiol, MMTS, formaldehyde, sulfonic and formic acids, together with DMDS in greater yields. The main products, DMSO and $DMSO_2$, arise from S oxidation.

It is well known that singlet oxygen (produced by energy transfer, Eqs. (4)–(5)) [37] or superoxide anion (produced by electron transfer, Eqs. (6)–(7)) [18,26,33] photosensitized oxidation of sulfides may give rise, besides the main sulfoxide product, to detectable amounts of sulfone and disulfide. Anthraquinone is, moreover, able to oxidize DMDS in MMTS [27]. DTP was already reported by Balla and Heicklen [38] as a product of the gas-phase photolysis of methanethiol or DMDS at short wavelength (254 nm) in the presence of oxygen, and its formation was assumed to occur by the way of oxygenated radicals $CH_3S(O)_2^{\bullet}$ and $CH_3SO_4^{\bullet}$.

From the low yields of these products, it can thus be assumed that with the photosensitizer-loaded materials used in this study, and contrary to TiO_2, the radical-cation $CH_3SCH_3^{\bullet+}$ is not the only involved intermediate. In turn, superoxide $O_2^{\bullet-}$ is probably not the reactive oxygen species as it can only result from a second electron transfer from the photosensitizer radical-anion $DCA^{\bullet-}$ or $ANT^{\bullet-}$ to ground-state oxygen (Eq. (7)) after the initial formation of the ion pair $CH_3SCH_3^{\bullet+}$, $Sens^{\bullet-}$ (Eq. (6)). These assumptions leave singlet oxygen as the main reactive oxygen species in the gas-phase photosensitized oxidation of dimethylsulfide with DCA and ANT, in agreement for the former with the results of a mechanistic investigation by Baciocchi et al. [33] However, further experiments are obviously needed to definitely conclude on this point; the comparison with TiO_2 derived products under strictly similar conditions should be helpful.

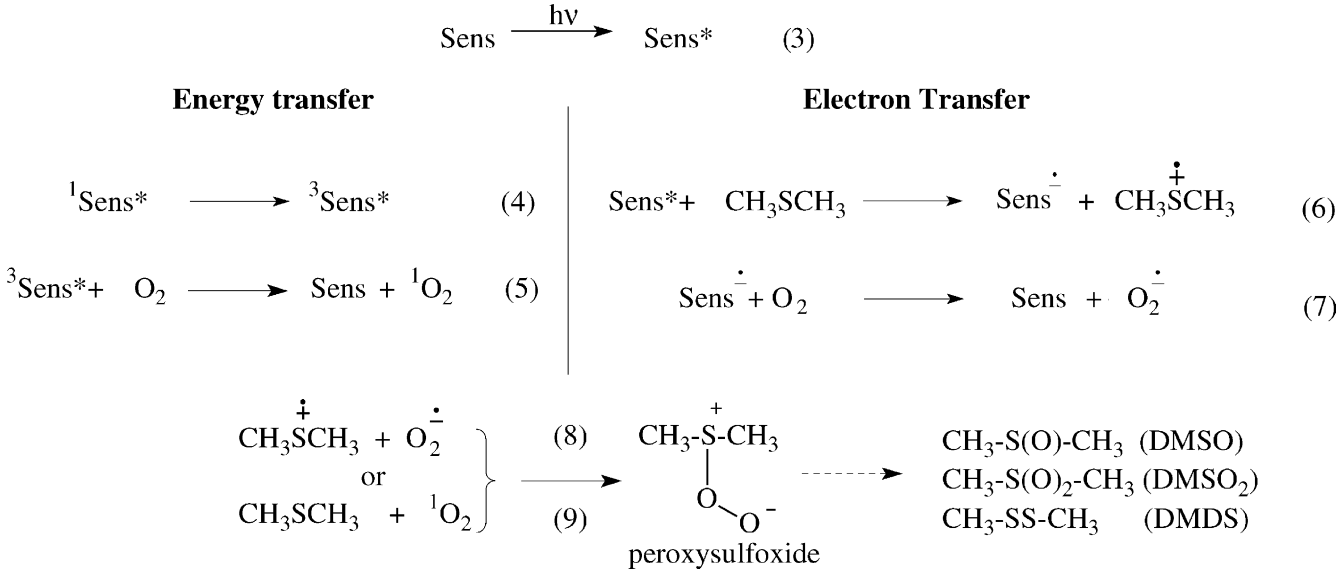

5. Conclusion

We have demonstrated that aromatic photosensitizers, such as DCA or ANT, when deposited (commercial beads) or included (monolithic sol–gels) in silica-materials, efficiently achieve gas-phase oxidation of dimethylsulfide, with oxygen as reactant under visible light in a single-path flow reactor. In the case of the most efficient DCA-based materials, the concentration of the photosensitizer has to be low enough (around 10^{-7} mol g^{-1}) in order to avoid deactivation through excimer formation. From the main detected oxidation products (sulfoxide, sulfone and disulfide), involvement of singlet oxygen may be assumed although further studies are needed to clarify this point. In any case, formation of reactive oxygen species at the gas–solid interface is demonstrated.

With regard to the photo-oxidative efficiency, our results also point out the influence of the properties of the silica support itself, such as transparency, homogeneity and specific surface area. The adsorption capacity of the material is a crucial parameter as the most DMS adsorbing material, DCA-SG, is also the most efficient with the highest turnover number.

Our materials thus display several advantages relative to TiO_2: first they are activated by visible light, and second they act as very efficient traps for partially oxidized products. Accordingly, the gas flow at the outlet of the photocatalytic device is free of any toxic or nauseous product for several days, contrary to the case of experiments with TiO_2-based materials.

As soon as products appear in the gas flow, the catalyst appears to be deactivated, but the silica beads can be easily regenerated by mild thermal treatment under controlled conditions, as demonstrated by their DRUV or fluorescence spectra. Accordingly, several runs adsorption–irradiation–heating could be achieved with these beads. For the sol–gel monoliths, the behaviour of the photosensitizer in the porous network during the reaction has to be quantitatively analysed, as well as the possibility to regenerate the material by washing in suitable solvents.

The design of photoactive, highly porous and transparent monoliths by sol–gel synthesis appears to bear promising developments for the treatment of gaseous pollutants. This preliminary work, which demonstrates the feasibility of gas–solid photo-oxidation reactions, opens the way to new kinds of materials, loaded with other photosensitizers with different properties and absorption spectra, designed for specific pollutants oxidation. In order to achieve a better stability of the photosensitizer on the inorganic support, its incorporation as a triethoxysilyl derivative during the sol–gel synthesis is currently considered and should lead to photosensitising ORMOSIL materials. The stability of the material under irradiation can be controlled by spectroscopic methods and suitable regeneration conditions have to be sought in order to make such materials competitive for decontamination of polluted atmosphere.

Acknowledgements

The authors thank F. Benoit-Marquié and M. T. Maurette (UMR CNRS 5624, POM group of IMRCP, Toulouse) for the design, realisation and gift of the diffusion cell.

The funding of AIR LIQUIDE Company is greatly acknowledged. During the course of this study, some antibacterial tests had been carried out by AIR LIQUIDE with the described materials.

References

[1] E. Blosseys, D. Neckers, J. Am. Chem. Soc. 95 (1973) 5820.
[2] L. Horner, J. Klaus, Liebigs Ann. Chem. (1981) 792.
[3] B. Paczkowska, J. Paczkowski, D. Neckers, Macromolecules 19 (1986) 863 (and related references).
[4] M. Nowakowska, M. Kepczynski, K. Szczubialka, Pure Appl. Chem. 73 (2001) 491.
[5] R. Alcantara, L. Canoira, P. Guilherme Joao, J. Gonzalo Rodriguez, I. Vasquez, J. Photochem. Photobiol. A: Chem. 133 (2000) 27.
[6] A. Riva, F. Trifiro, F. Santarelli, J. Mol. Catal. 11 (1981) 283.
[7] A. Jensen, C. Daniels, J. Org. Chem. 68 (2003) 207.
[8] J. Bourdelande, J. Font, F. Sanchez-Ferando, Tetrahedron Lett. 21 (1980) 3805.
[9] J. Bourdelande, J. Font, F. Sanchez-Ferrando, Can. J. Chem. 61 (1983) 1007.
[10] V. Iliev, A. Ileva, L. Bilyarska, J. Mol. Catal. A: Chem. 126 (1997) 99.
[11] R. Gerdes, O. Bartels, G. Schneider, D. Wöhrle, G. Schulz-Ekloff, Polym. Adv. Technol. 12 (2001) 152.
[12] M. Suzuki, Y. Ohta, H. Nagae, T. Ichinohe, M. Kimura, K. Hanabusa, H. Shirai, D. Wöhrle, Chem. Commun. (2000) 213.
[13] D. Wöhrle, A. Khezr Sobbi, O. Franke, G. Shulz-Ekloff, Zeolites 15 (1995) 540.
[14] M. Miranda, A. Amat, A. Arques, Catal. Today 76 (2002) 113.
[15] A. Sanjuan, M. Alvaro, G. Aguirre, H. Garcia, J. Scaiano, J. Am. Chem. Soc. 120 (1998) 7531.
[16] J. Mattay, M. Vondenhof, R. Denig, Chem. Ber. 122 (1989) 951.
[17] M. Ayadim, J.P. Soumillion, Tetrahedron Lett. 36 (1996) 381.
[18] N. Soggiu, H. Cardy, J.L. Habib-Jiwan, I. Leray, J.Ph. Soumillion, S. Lacombe, J. Photochem. Photobiol. A: Chem. 124 (1999) 1.
[19] M. Julliard, in: M. Chanon (Ed.), Homogeneous Photocatalysis, John Wiley and Sons Ltd., 1997, p. 222.
[20] D. Latassa, O. Enger, C. Thilgen, T. Habicher, H. Offermans, F. Diederich, J. Mater. Chem. 12 (2002) 1993.
[21] A. Zeug, J. Zimmermann, B. Röder, M. Lagorio, E. San Roman, Photochem. Photobiol. Sci. 1 (2002) 198.
[22] R. Nilsson, D. Kearns, Photochem. Photobiol. 19 (1974) 181.
[23] T. Tanaka, H. Nojima, T. Yamamoto, S. Takenaka, T. Funabiki, S. Yoshida, Phys. Chem. Chem. Phys. 1 (1999) 5235.
[24] J. Peral, X. Domenech, D. Ollis, J. Chem. Technol. Biotechnol. 70 (1997) 117.
[25] M. Lewandowski, D. Ollis, Mol. Supramol. Photochem. (Semiconductor Photochem. Photophys.), 10 (2003) 249.
[26] S. Lacombe, H. Cardy, M. Simon, A. Khoukh, J.Ph. Soumillion, M. Ayadim, Photochem. Photobiol. Sci. 1 (2002) 357.
[27] V. Latour, T. Pigot, M. Simon, H. Cardy, S. Lacombe, Photochem. Photobiol. Sci. 4 (2005) 221.
[28] S. Lacombe, H. Cardy, N. Soggiu, S. Blanc, J.L. Habib-Jiwan, J.Ph. Soumillion, Microporous Mesoporous Mater. 46 (2001) 311.
[29] F. Benoit-Marquié, M.T. Boisdon, A.M. Braun, E. Oliveros, M.T. Maurette, Entropie 228 (2000) 36.
[30] F. Benoit-Marquié, Ph.D. Thesis, University Paul Sabatier, Toulouse, 1997.

[31] Y. Grillet, P. Llewellyn, in: A.P. Legrand (Ed.), The Surface Properties of Silica, Wiley, Chichester, 1999, p. 23.
[32] N. Serpone, A.V. Emeline, Int. J. Photoenergy 4 (2002) 91.
[33] E. Baciocchi, T. Del Gaccio, F. Elisei, M.F. Gerini, M. Guerra, A. Lapi, P. Liberali, J. Am. Chem. Soc. 125 (2003) 16444.
[34] K. Gollnick, S. Held, J. Photochem. Photobiol. A: Chem. 70 (1993) 135.
[35] A. Alegria, A. Ferre, G. Santiago, E. Sepulveda, W. Flores, J. Photochem. Photobiol. A: Chem. 127 (1999) 57.
[36] A. Vorontsov, E. Savinov, L. Davydov, P. Smirniotis, Appl. Catal. B: Env. 32 (2001) 11.
[37] E. Clennan, Acc. Chem. Res. 34 (2001) 875.
[38] R. Balla, J. Heicklen, J. Photochem. 29 (1985) 311.